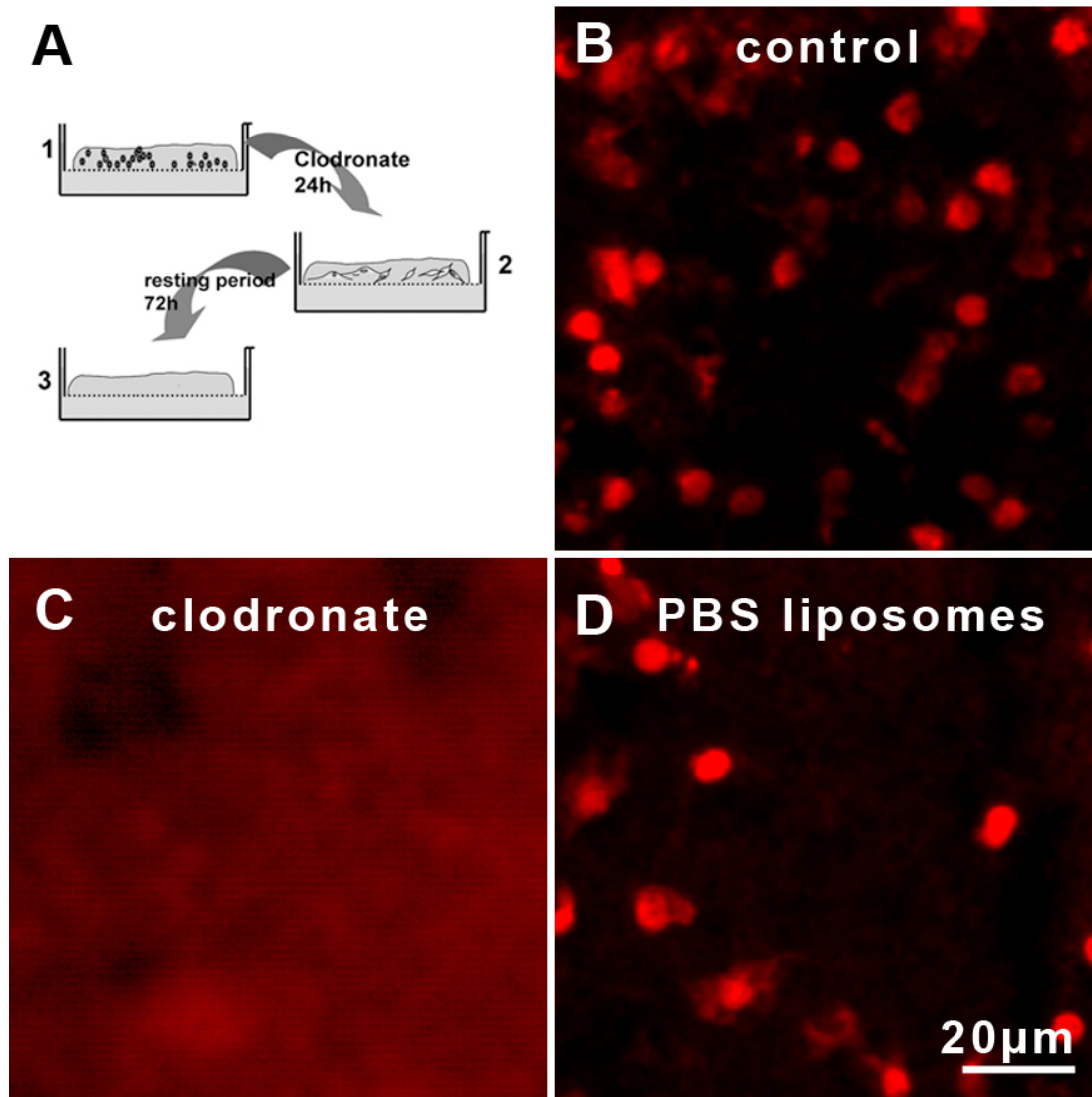


### **3. Results**

#### **3.1. Characterization of the glioma experimental model**

##### **3.1.1. Organotypical brain slice cultures can be selectively depleted of microglia**

To study the impact of microglia on tumor invasion, we developed a protocol to deplete microglia from organotypic brain slice cultures (Fig. 3.1A). This method allowed us to inoculate glioma cells into microglia-free tissue and compare their invasive potential to control tissue. Fig. 3.1B-D shows fluorescence micrographs of Iba-1 labeled microglia of organotypical brain slice cultures cryosections. In untreated organotypical brain slice cultures, microglial cells were evenly distributed within the tissue when inspected 96h after plating. The microglia exhibit mainly amoeboid and to a lesser extent ramified morphology, indicating a certain level of microglial activation in organotypical brain slice cultures (Fig. 3.1B). Treatment of organotypical brain slice cultures for 24h with clodronate liposomes and a subsequent 72h culturing period without clodronate liposomes resulted in complete depletion of microglial cells (Fig. 3.1C). Application of liposomes filled with buffer alone (PBS-liposomes) did not result in depletion of microglia under identical experimental conditions (Fig. 3.1D). However, an uneven distribution of Iba 1-positive cells was observed in vertical sections. Within 24 h, microglial cells accumulated close to the surface of the brain slice and were amassed around blood vessels.



**Fig. 3.1. Microglia are depleted in cultured brain slices after clodronate liposome treatment.** (A) The procedure for microglia depletion is illustrated: in a first step the tissue is depleted of microglia by culturing acutely isolated slices in a transwell format delivering clodronate liposomes with the medium for 24h; secondly, the medium was exchanged to liposome-free conditions and cultured for an additional 72h, to allow astrocytes to restore resting GFAP levels. (B-D) Fluorescence micrographs of microglia distribution in cryosections obtained from a organotypical brain slice cultures (96h in culture) labelled with Iba-1 antibody. (B) Note the even and widespread distribution of microglia. Microglia exhibit mainly amoeboid and to a lesser extent ramified morphology. Whole brain slices were labeled for microglia using Iba-1 antibodies. (C) Microglia is virtually undetectable in brain slices treated 24h with clodronate liposomes and subsequently cultured for 72h in normal culturing medium. (D) Distribution of microglia in brain slices exposed to PBS-liposomes.

To investigate the distribution of microglia throughout the entire organotypical brain slice cultures, two-photon microscopy was used. After 96h in culture, microglia were present at the surface, center and bottom of the slice as identified with IL-B4 labeling

(Fig. 3.2A). On the contrary, in clodronate liposome treated organotypical brain slice cultures there was no detectable microglia (Fig. 3.2B). However, blood vessels were still labeled by IL-B4.

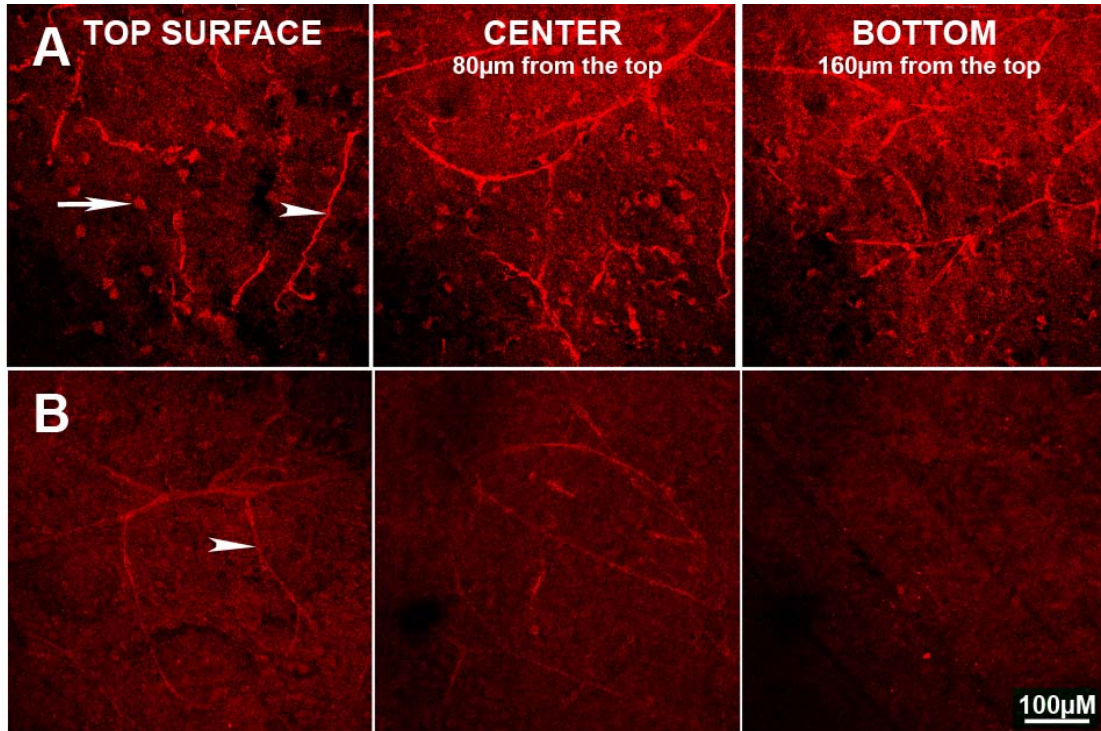


**Fig. 3.2. Microglia is present and equally distributed in organotypical brain slice cultures and absent in organotypical brain slice cultures treated with clodronate liposomes.** Organotypical brain slice cultures were treated with clodronate liposomes for 24h and then cultivated for additional 72h. Then slices were labeled with IL-B4 conjugated with the Texas red fluophore (labeling microglia as well as endothelial cells). (A) IL-B4 clearly labeled microglia (arrow) and blood vessels (arrowhead). Two-photon microscopy revealed the presence of microglia at the surface, in the middle and at the bottom of the control organotypical brain slice cultures. The microglia mostly exhibited amoeboid morphology. (B) In the clodronate liposome treated organotypical brain slice cultures, microglia was not detectable, whereas the blood vessels were still present (arrowhead).

### 3.1.2. Organotypical brain slice cultures and GL261 glioma cells remain viable after clodronate liposome treatment

Toxicity of clodronate liposome treatment on organotypical brain slice cultures or GL261 cells was tested with Calcein AM and Ethidium homodimer stains ('Live-Dead kit'). Live cells are distinguished by the presence of ubiquitous intracellular esterase activity, determined by the enzymatic conversion of the nonfluorescent cell-

permeant calcein AM to the fluorescent calcein. The polyanionic dye calcein is well retained within live cells, producing an intense uniform green fluorescence in live cells (ex/em ~495 nm/~515 nm). The ethidium homodimer enters cells with damaged membranes and undergoes a 40-fold enhancement of fluorescence upon binding to nucleic acids, thereby producing a bright red fluorescence in dead cells (ex/em ~495 nm/~635 nm). The ethidium homodimer is excluded by intact plasma membranes of live cells. The organotypical brain slice cultures were routinely checked for apoptosis after treatment with clodronate liposomes at different time points and the number of living and dead cells was counted with a fluorescence microscope and there was no statistical difference between control organotypical brain slice cultures to clodronate liposome treated organotypical brain slice cultures. Moreover, GL261 cells did not show an increase in cell death after clodronate liposome treatment as assessed by the 'Live-Dead' kit (Fig. 3.3.). The number of dead GL261 cells in control and clodronate liposome treated for 24h was similar and constantly very low with 2-3% of dead cells.

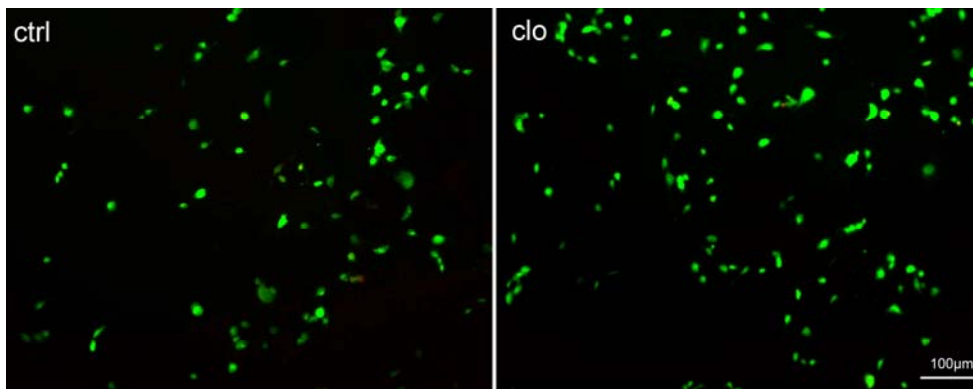


**Fig. 3.3. Clodronate liposome treatment does not alter cell death in GL261 cells.** GL261 cells were cultured 24h with a medium containing 10% clodronate liposomes, and subsequently labeled with calcein/ethidium homodimer stains. Maximally 3% of cells from 3 independent experiments were stained with the ethidium homodimer indicating dead cells.

### **3.1.3. Astrocytes and neurons are not affected by clodronate treatment**

To test the impact of the clodronate liposome treatment on astrocytes, transgenic mice were used in which astrocytes are expressing enhanced green fluorescent protein (EGFP) under a promoter for glial fibrillary acidic protein (GFAP). If neurons supported the clodronate liposomes treatment it was investigated in normal, wild type (wt) C57/BL6 mice. GFAP and neurofilament-200 immunocytochemistry was used to identify astrocytes and neurons, respectively. EGFP expression in GFAP-EGFP transgenic mice increases when the astrocytes are activated (Nolte, Matyash et al. 2001) and therefore represents an indicator of astrocytic activation. Organotypical brain slice cultures from GFAP-EGFP transgenic mice also express low amounts of EGFP under control conditions (Fig. 3.4A), but this increased significantly within the first 24h after clodronate liposome treatment (Fig. 3.4B). 72h after treatment with clodronate liposomes (96h in culture), control and clodronate treated organotypical brain slice cultures were indistinguishable with respect to GFAP expression (Fig. 3.4 C-D). Additionally, the astrocytic morphology in control or clodronate treated organotypical brain slice cultures (obtained from C57 wt mouse) was revealed by labeling with the GFAP antibody. After 96h in culture, there were no detectable differences in GFAP expression and cell morphology in organotypical brain slice cultures of control or clodronate liposomes treated organotypical brain slice cultures (Fig. 3.5A-B). A characteristic, fine, filamentous morphology of astrocytes was detected in both, control and clodronate liposome treated organotypical brain slice cultures (Fig. 3.5A-B). Thus, astrocytes within the slice preparations survived the clodronate treatment without attenuation of their ability to respond to external stimuli. Neuronal labeling by neurofilament-200 (NF 200) after 96h in culture did not differ in control versus clodronate liposomes treated organotypical brain slice cultures as revealed by confocal microscopy of brain slices (Fig. 3.5C-D). Therefore organotypical brain slice cultures were inoculated for 72h after clodronate liposome treatment to avoid an influence of reactive astrocytes on the tumor implants.

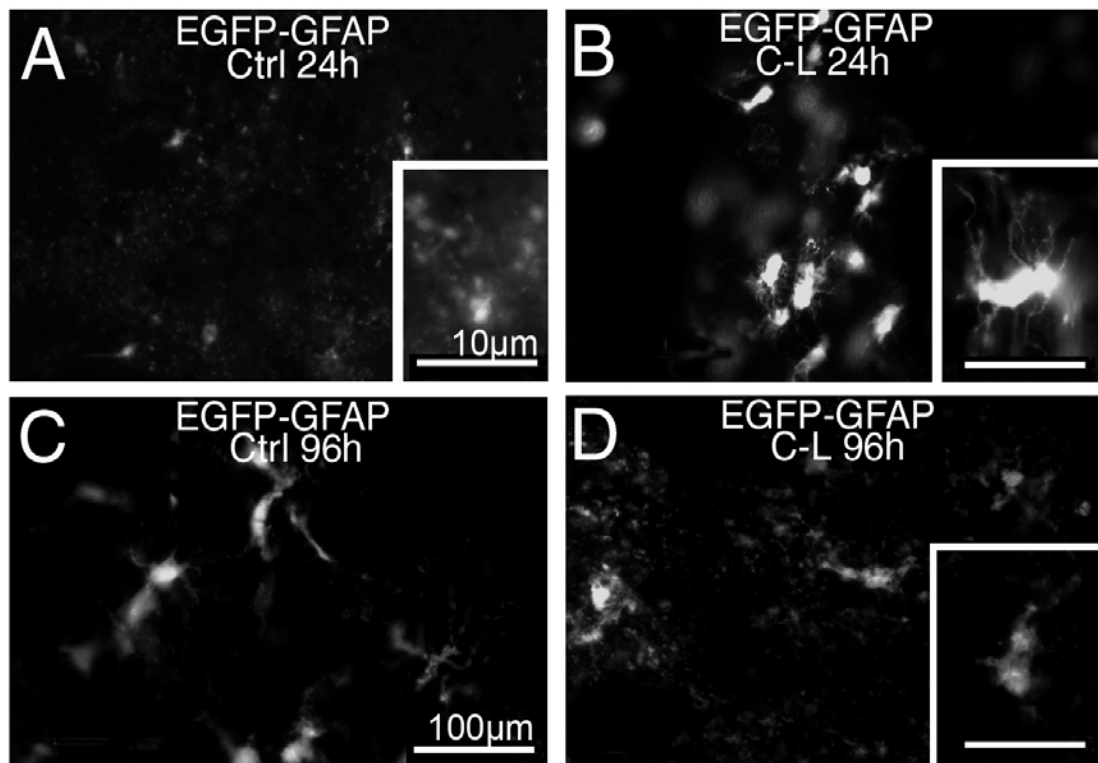


**Fig. 3.4. Astrocytes are in a resting state 72h after clodronate liposome treatment of organotypical brain slice cultures.** Astrocytes were labeled by EGFP expression in the EGFP-GFAP transgenic mouse. (A) Fluorescence image of EGFP expression in a control organotypical brain slice cultures treated for 24h with PBS-filled liposomes. A single astrocyte is depicted in the insert. (B) EGFP labeling of a organotypical brain slice cultures after 24 h treatment with clodronate liposomes indicates the upregulation of GFAP. Note the branched morphology and the intense fluorescence of the individual activated astrocytes as compared to the control in (A). A single astrocyte is shown at higher magnification in the insert. (C, D) Images of EGFP fluorescence 72h after treatment with PBS (C) or clodronate filled liposomes (D). The EGFP fluorescence is similar in both images and resembles the control 24h after treatment as shown in (A). Note the low fluorescence of an individual resting astrocyte in the insert in (D).

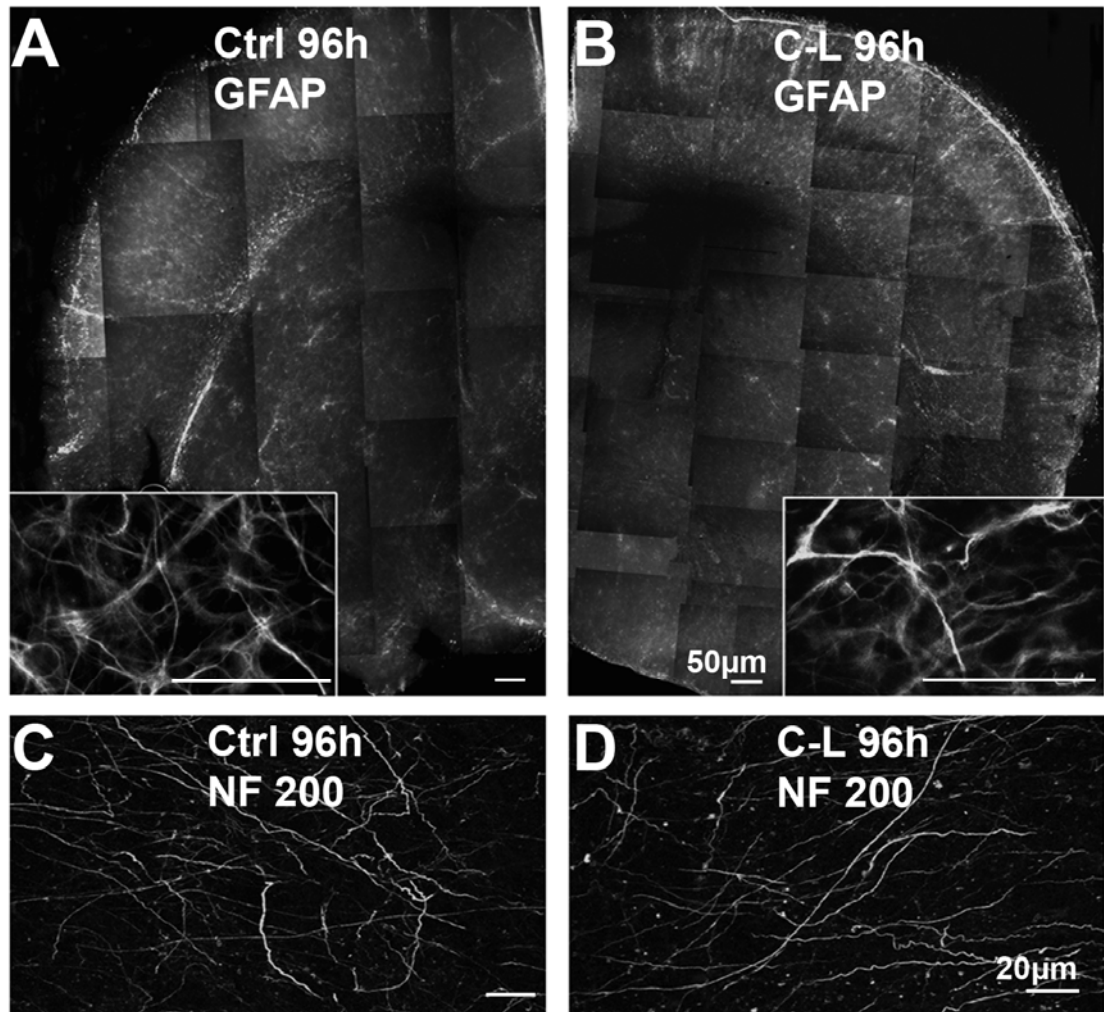


**Fig. 3.5. Morphology of astrocytes and neurons in organotypical brain slice cultures remain unchanged after clodronate liposome treatment.** (A-B) Single images taken by fluorescence microscopy were merged to large composites giving an overview on the distribution of GFAP after 96h in culture. The GFAP expression is similar in control organotypical brain slice cultures (A) and 24h clodronate liposome treated organotypical brain slice cultures after additional 72h culturing (B). Note the branched morphology and long processes of astrocytes shown in inserts at higher magnification. (C-D) Neurofilament-200 (NF 200) immunoreactivity labels neurons after 96h in control brain slice culture (C) or clodronate liposome treated culture (D).

### **3.1.4. Tumor cell migration can be quantified after inoculation of glioma cells into cultured brain slices**

To establish a reproducible model for tumor cell migration, approximately 5000 EGFP transfected F98 or GL261 tumor cells were inoculated into the slices. 2 h after injection, the EGFP-labeled glioma cells were concentrated within less than 300  $\mu\text{m}$  from the injection canal (n=8, not shown). An example from a single experiment is shown in (Fig. 3.6A-E). Over a time course of 5 days, we observed and quantified the migration of glioma cells away from the injection site. The organotypical brain slice cultures flattened during the culture period to a thickness of about 150  $\mu\text{m}$ . The highest glioma cell density was consistently detected in the center of the organotypical brain slice culture. To evaluate tumor cell invasion we measured the distance between the individual fluorescent cells and the center of the injection canal. To quantify tumor cell migration we measured the distance, which fluorescent cells traveled from the center of the injection canal (Fig. 3.6D). 24h after inoculation the GL261 cells were found within a radius of up to 500 $\mu\text{m}$ , after 48 h some cells had migrated beyond this distance. After 96 h and 120 h, the majority of tumor cells had migrated beyond 500 $\mu\text{m}$  from the injection site in control organotypical brain slice culture (Fig. 3.6F), in contrast to microglia depleted organotypical brain slice cultures (Fig. 3.6G). Accumulated data from up to 600 cells per injection site allowed us to assemble distance histograms (Fig. 3.6F-G)

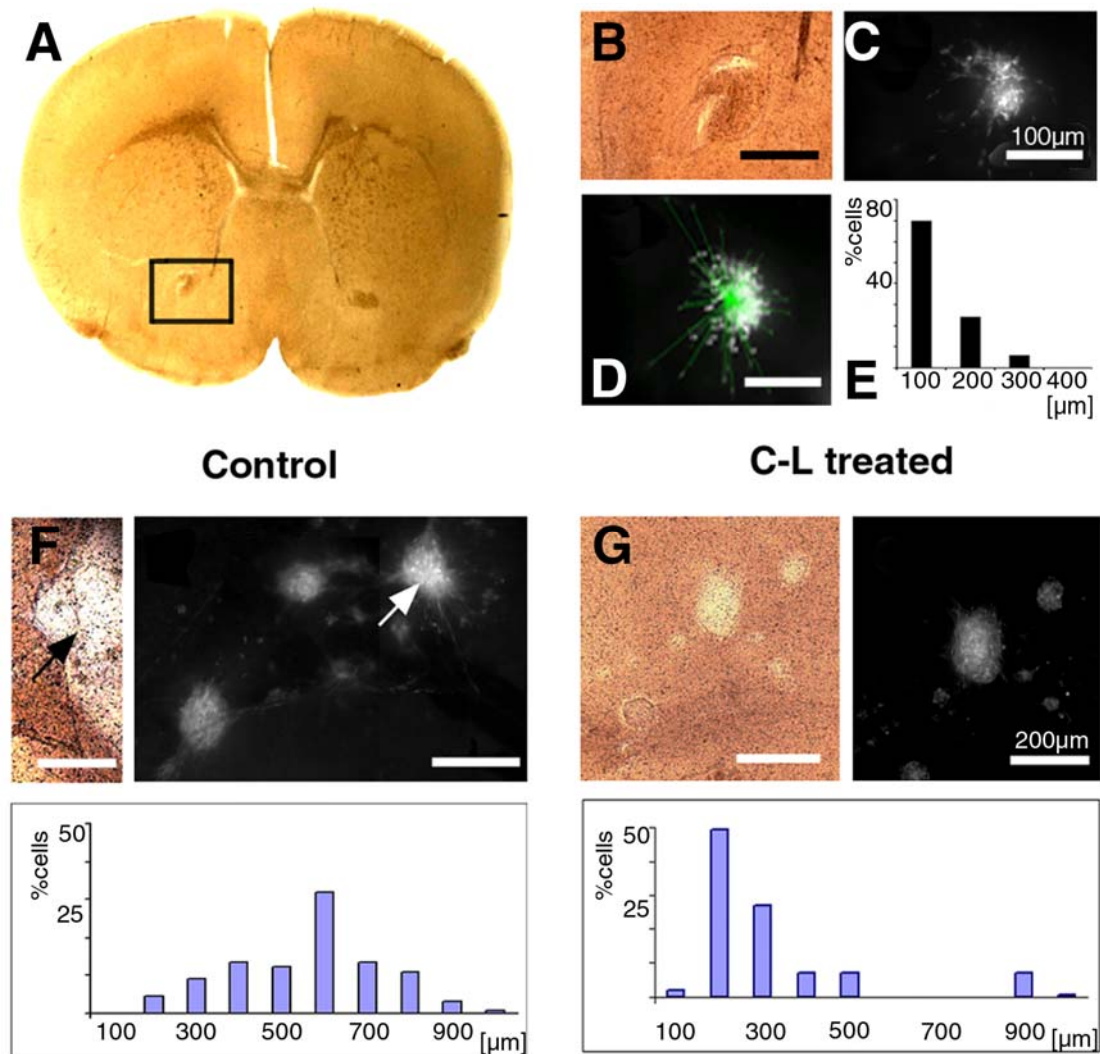


**Fig. 3.6. Detection of glioma cells inoculated into cultured brain slices.** (A) The phase contrast image shows a brain slice 2h after inoculation with glioma cells. The tumor is located in the area highlighted by the square. (B) A magnified image of the square field in (A). (C) A confocal fluorescence image shows the EGFP labeled glioma cells of the area depicted in (B). (D) The distance of individual glioma cells is determined with the Image Pro software. The measured distances are superimposed to the image shown in (C). (E) A distance histogram was constructed, from the distances measured in (D). Note that the majority of cells had migrated less than 300 $\mu$ m. (F-G) A phase contrast (left) and a confocal fluorescence image (right) from glioma cells containing control organotypical brain slice culture (F) and clodronate treated organotypical brain slice culture (G) after 4 days in culture. The arrows in the phase contrast and confocal micrographs are indicating corresponding areas of the tumor. The histogram points out the distance the tumor cells traveled from the tumor center.

### 3.1.5. Experimental gliomas in organotypical brain slice cultures share features with human glioblastomas

First, we evaluated if our experimental model exhibits associations of microglia with glioma cells that are similar to those reported for human glioblastomas. Second, I studied which invasion pattern the glioma cells would show in this model, i.e. do glioma cells invade as single cells or as cell-clusters and do they diffusely infiltrate the parenchyma or progress along blood vessels. 4 days post implantation microglia had infiltrated the tumors and aggregated in large numbers around the tumors (as determined by labeling with the microglia marker Iba 1; Fig. 3.7A). At this timepoint, the highly invasive glioma cells, which are distant to the injection site, are either found as single cells or as groups of a few cells within the parenchyma (Fig. 3.7A-B). Labeling for the endothelial cell marker von-Willebrand-factor revealed that a fraction of glioma cells was closely associated with blood vessels (Fig. 3.7B).

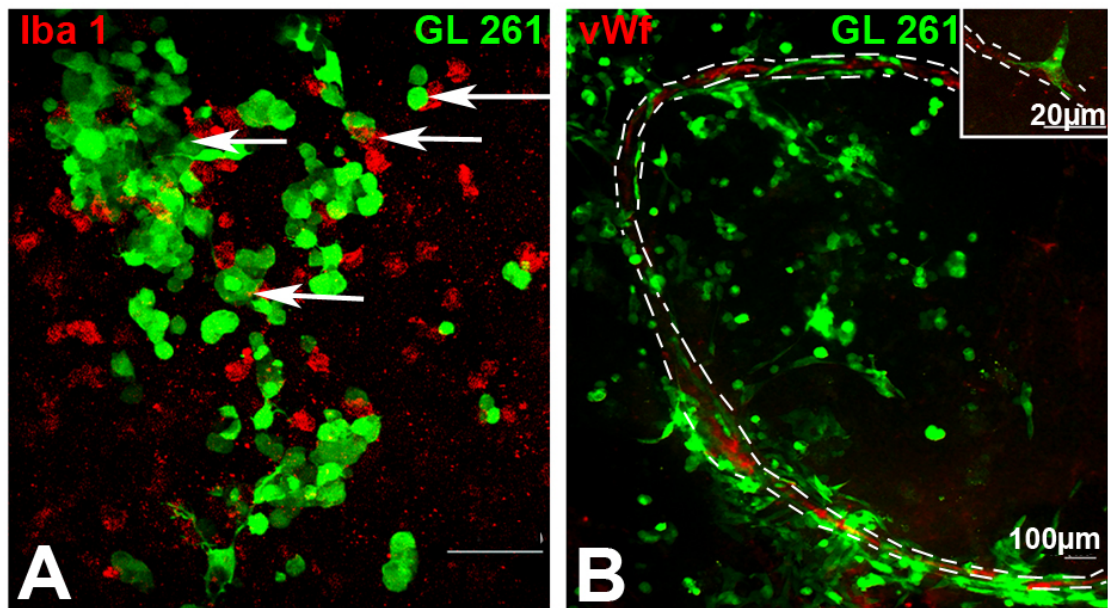


**Fig. 3.7. Attributes of human glioblastomas are reflected in organotypical brain slice cultures experimental gliomas.** (A) A confocal microscopy image of organotypical brain slice cultures shows Iba 1 immunolabeled microglia (red) associating with GFP labeled glioma cells (green) in organotypical brain slice cultures. Note the close association between microglia and glioma cells (arrows). (B) GL261 are close to a blood vessel labeled with vWf antibody (red). GL261 appeared to move along blood vessels (delineated with dashed lines). The insert illustrates a glioma cell close to a blood vessel. Note that some glioma cells are not in close association with blood vessel.

### **3.2. Glioma invasion directly correlates with microglia density**

#### **3.2.1. In microglia-depleted organotypical brain slice cultures glioblastoma cell invasion is impaired**

We compared tumor cell migration in untreated control organotypical brain slice cultures, or cultures treated with PBS-filled liposomes and microglia depleted organotypical brain slice cultures at days 2, 4 and 5 after F98 or GL261 cell injection. 2 days after injection, the bulk population of glioma cells formed a tumor mass of approximately 500  $\mu\text{m}$  in radius and only few cells dispersed out of this mass (Fig. 3.8A). To get a measure of the migratory potential of the tumor cells, we arbitrarily defined two cell populations. A first population, which stayed within a radius of 500 $\mu\text{m}$  to the tumor center was regarded as resident cells. A second cell population, which had migrated beyond that radius are referred to as invasive cells. At day 2 after tumor inoculation there was no significant difference in migratory distances in untreated compared to microglia depleted organotypical brain slice cultures. The distribution of GL261 cells throughout the organotypical brain slice cultures in control and clodronate liposomes treated groups were similar (Fig. 3.8A and D). In control organotypical brain slice cultures 9% of cells migrated more than 500 $\mu\text{m}$ , compared to microglia depleted organotypical brain slice cultures where 12% of GL261 cells migrated more than 500 $\mu\text{m}$ , (Fig. 3.8D). Similarly, 19% F98 glioma cells had migrated more than 500 $\mu\text{m}$  in control and 12% in microglia depleted organotypical brain slice cultures (Fig. 3.28E). 4 days post-inoculation, the difference in migratory distances in normal and microglia depleted organotypical brain slice cultures became apparent with both cell lines. With GL261 cells 44% migrated more than 500 $\mu\text{m}$  in untreated organotypical brain slice cultures and 33% in microglia depleted organotypical brain slice cultures (Fig. 3.8B and D). The population of F98 cells which migrated more than 500 $\mu\text{m}$ , consisted of 52% in control organotypical brain slice cultures and 23% in microglia depleted organotypical brain slice cultures (Fig. 3.8E). 5 days after inoculation the difference in invasiveness of glioma cells between microglia depleted and non-depleted groups remained (Fig. 3.8C). In untreated organotypical brain slice cultures 67% of GL261, and 66% of F98 cells invaded more than 500 $\mu\text{m}$  (Fig. 3.8D and E). In microglia depleted organotypical brain slice cultures, the population of invasive cells was significantly lower. 43% of GL261 and 49% of F98 migrated more than 500 $\mu\text{m}$  (Fig. 3.8D and E). Hence, both

glioma cell lines revealed decreased invasiveness in the microglia-depleted organotypical brain slice cultures as compared to controls.

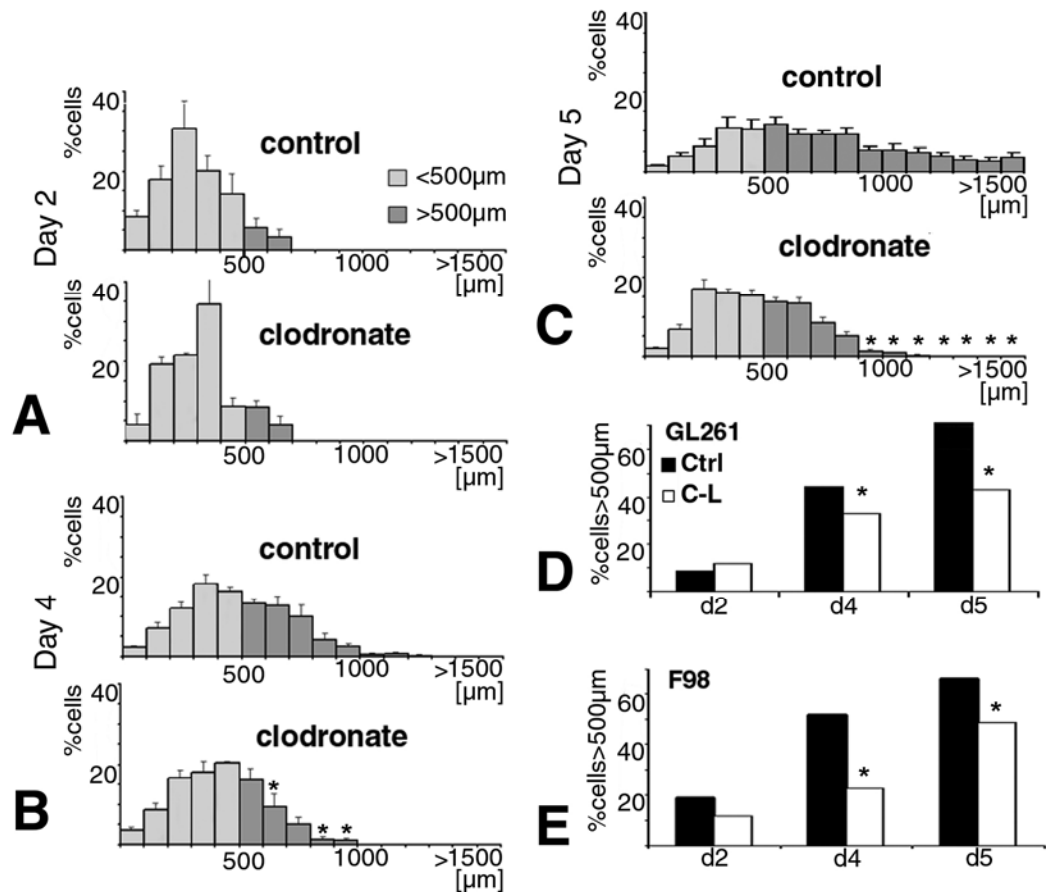


**Fig. 3.8. GL261 and F98 cells are more invasive in normal (control) organotypical brain slice cultures as compared to microglia depleted organotypical brain slice cultures.** (A-C) The migration of glioma cells within organotypical brain slice cultures was determined and distance histograms were constructed as described in the legend to Fig. 3.6. The upper histogram is an average from at least 16 independent experiments from control respectively microglia depleted organotypical brain slice cultures 2 days (A), 4 days (B) and 5 days (C) after glioma inoculation. (D, E) The histograms are obtained from data shown in (A-C) and indicate the percentage of cells which migrated  $>500 \mu\text{m}$  in control (Ctrl) and clodronate liposomes treated slices for GL261 (D) and F98 (E) cells. Asterisks are indicating statistical significance ( $p < 0,05$ ) between the control organotypical brain slice cultures and clodronate liposome treated groups.

In organotypical brain slice cultures treated with PBS filled liposomes, we observed a migratory behavior for both cell lines that was consistently in between the values obtained for microglia-depleted and control organotypical brain slice cultures (not shown). This intermediate invasiveness is probably due to the accumulation of

microglia in certain areas of the slices e.g. around blood-vessels and at the edges of the organotypical brain slice cultures, which left other regions of the organotypical brain slice cultures largely depleted of microglia, as illustrated in (Fig. 3.1.).

### **3.2.2. Co-injection of microglia and gliomas promotes invasion of glioma cells**

To further establish that microglia promote tumor migration, microglia were co-injected with the glioma cells into organotypical brain slice cultures. 5 days after inoculation we compared organotypical brain slice cultures containing 5000 GL261 cells with those that were co-injected with 5000 GL261 cells and 5000 microglial cells. In control organotypical brain slice cultures, 33% remained within 500  $\mu\text{m}$  from the injection canal (Fig. 3.9A), compared to 17% in co-injected organotypical brain slice cultures (Fig. 3.9B). Moreover, in co-injected organotypical brain slice cultures we observed a substantially elevated fraction of tumor cells invading very far (1500 $\mu\text{m}$  and more) into the organotypical brain slice cultures preparation.

It was also investigated in how far the co-injected microglia may have impact on glioma migration in microglia depleted organotypical brain slice cultures. The fraction of invading glioma cells was again lower in clodronate liposomes treated organotypical brain slice cultures (44%, Fig. 3.9C compared to 67% in non-depleted organotypical brain slice cultures, Fig. 3.9A). Only a few cells migrated beyond 1500 $\mu\text{m}$ . When microglia was injected together with glioma cells into previously microglia depleted organotypical brain slice cultures, 75% of the glioma cells were found beyond 500 $\mu\text{m}$  and significantly more cells were found beyond 1500 $\mu\text{m}$  (Fig. 3.9D and E). These experiments demonstrate that microglial cells promote tumor invasion.

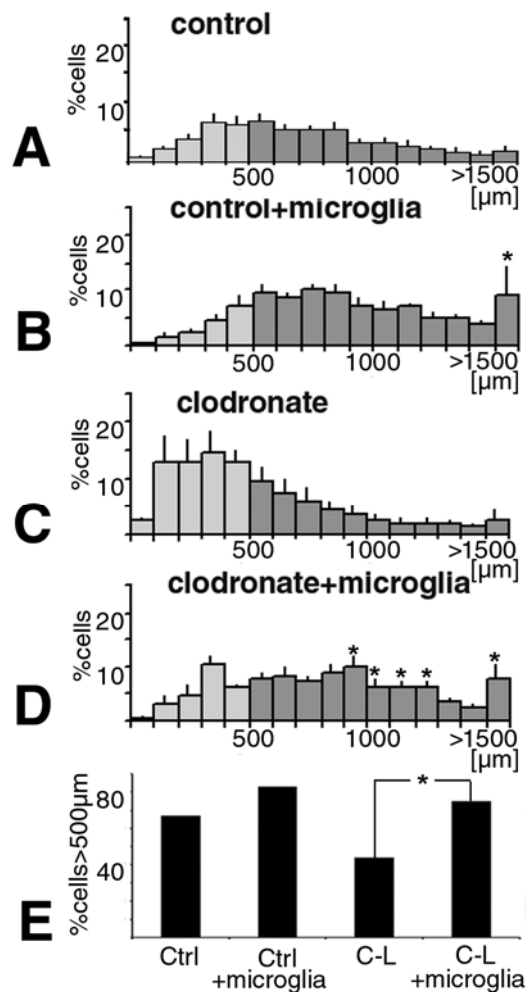


**Fig. 3.9. Density of microglial cells correlates with increased invasive potential of glioblastoma cells.** The migration of glioma cells within organotypical brain slice cultures was determined and distance histograms were constructed as described in the legend to Fig 3.6. The histograms are averages from at least 10 independent experiments. Control slices (A, B) and clodronate treated slices (C, D) were compared 5 days after injection of glioma cells (A, C) or co-injection of glioma cells with microglial cells (B,D). (E) The percentage of cells that had migrated more than 500 μm are displayed in the histogram as obtained from data shown in (A-D). Ctrl, corresponds to (A), Ctrl + microglia to (B), clodronate liposomes to (C) and clodronate liposomes+microglia to (D). Asterisks are indicating statistical significance ( $p < 0,05$ ) between the groups.

### **3.2.3. LPS stimulation does not increase glioma invasiveness in organotypical brain slice cultures**

The number of microglia in the glioma vicinity directly correlates with glioma invasiveness (Fig. 3.8. and 3.9.). Moreover, microglia appear predominantly amoeboid in the direct vicinity to glioma (Fig. 3.7.) indicating a certain level of activation. To assess if the amoeboid morphology of microglia is associated with an increased “activation” of the monocytic cells, glioma bearing organotypical brain slice cultures were further stimulated with lipopolysaccharide (LPS) from Gram-negative bacteria walls. Treatment with 100ng/ml or 1µg/ml LPS did not increase GL261 migration in organotypical brain slice cultures. 96h after preparation the organotypical brain slice cultures were incubated with LPS for a period of 24h, then GL261 EGFP cells were injected and their migration was observed. Tumor sizes of glioma in organotypical brain slice cultures were measured (Fig. 3.10.) Augmented tumor sizes were used as an indicator for increased glioma invasiveness and increased glioma proliferation. Thus, in all three experimental paradigms (clodronate, PBS liposomes or control organotypical brain slice cultures) there was no difference in tumor size at the respective time points after LPS treatment. The tumors steadily increased under all three conditions. Constant stimulation of organotypical brain slice cultures with LPS throughout the whole experiment was toxic to the organotypical brain slice cultures.

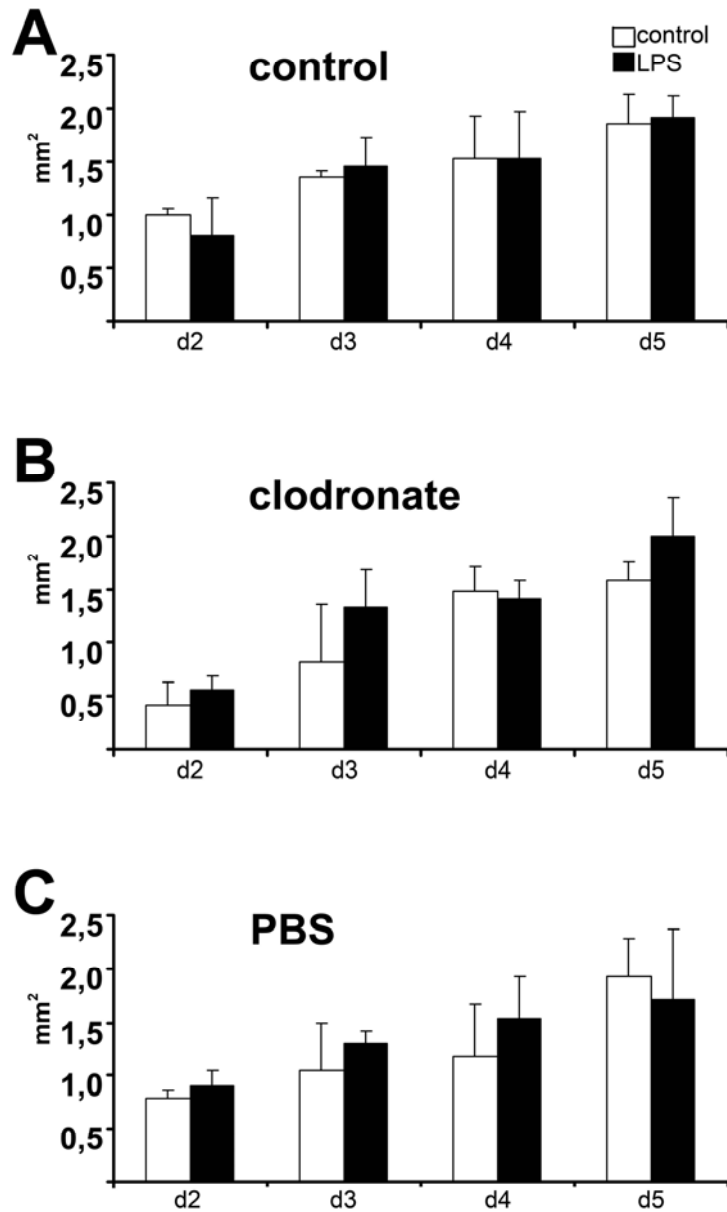


**Fig. 3.10. LPS treatment does not increase tumor size in organotypical brain slice cultures.** The organotypical brain slice cultures were treated with 100ng/ml LPS for 24h. Then, GL261- EGFP cells were injected and their invasiveness was evaluated by measuring the tumor surfaces. Tumor surface size was compared between control organotypical brain slice cultures - normally cultured slices (A), Clodronate (microglia depleted slices) organotypical brain slice cultures (B) and PBS (PBS filled liposome treated) organotypical brain slice cultures (C).

### **3.3. Microglia increases MMP-2 activation**

#### **3.3.1. Glioma induced MMP-2 activity is elevated in organotypical brain slice cultures containing microglia**

To monitor the activity of the metalloproteinases MMP-2 and MMP-9, extracts from organotypical brain slice cultures were analyzed by gelatin-zymography. In organotypical brain slice cultures inoculated with glioma for 5 days, prominent bands indicating proteolytic activity of MMPs were consistently observed at approximately 65kDa (Fig. 3.11A) while only faint bands appeared in the range of approximately 92kDa (not shown), demonstrating that the major activity is due to MMP-2 and not MMP-9. In microglia depleted and glioma bearing organotypical brain slice cultures, the activity of MMP-2 was considerably lower as compared to controls (Fig. 3.11A, left panel). In a different experiment exogenously cultured microglia was added together with the tumor into organotypical brain slice cultures. The MMP-2 activity in these organotypical brain slice cultures were profoundly elevated as compared to organotypical brain slice cultures receiving a glioma injection only (Fig. 3.11.A, right panel).

Next, I investigated the levels of MMPs, which are secreted from tumor bearing organotypical brain slice cultures that contain different densities of microglial cells. Supernatant from organotypical brain slice cultures 5 days after glioma inoculation was harvested and assayed in the zymogram. Control organotypical brain slice cultures without tumors displayed a baseline-level of MMP-2 activity, which was substantially increased in organotypical brain slice cultures inoculated with GL261 cells (Fig. 3.11.B, left part of the panel). However, in microglia depleted organotypical brain slice cultures inoculated with glioma, proteolysis by MMP-2 dropped to baseline levels.

When the microglia density in the tumor was elevated above control levels by co-inoculating exogenously cultured microglia and GL261 cells into organotypical brain slice cultures, MMP-2 activity increased substantially as compared to organotypical brain slice cultures containing tumors with normal density of microglia (Fig. 3.11.B). As described for zymograms from whole organotypical brain slice cultures extracts, faint bands displaying activity for MMP-9 were visible in those samples where microglia was present (not shown).

### **3.3.2. A soluble factor from glioma triggers the activation of MMP-2 in cultured microglial cells**

To investigate a cross-talk between glioma and microglial cells possibly influencing MMP-2 activity, a cell culture system was used in which GL261 cells were stimulated with microglia conditioned medium and vice versa. After over-night incubations the cells were washed and media were changed to serum free conditions, leaving the cells to liberate active MMP into the fresh medium. Prominent bands for active MMP-2 (at 65kDa) and for pro-MMP-2 (at 72kDa) were visible in zymograms from supernatants of unstimulated GL261 cells. This release activity by GL261 cells was not affected by microglia conditioned medium (Fig. 3.11C). Proteolysis by soluble MMP-2 released from microglial cells, which were kept under control conditions (not stimulated with GL261 conditioned medium) were at the detection limit of the zymogram assay. However, when microglia was incubated with glioma conditioned medium, the MMP-2 activity was strongly increased. Whereas zymograms from supernatants of GL261 cells showed bands for pro-MMP-2 and for activated MMP-2 under both experimental conditions, stimulation of microglia resulted only in the elevation of a very faint band for pro-MMP-2 but a strong band for active MMP-2 (Fig. 3.11C).

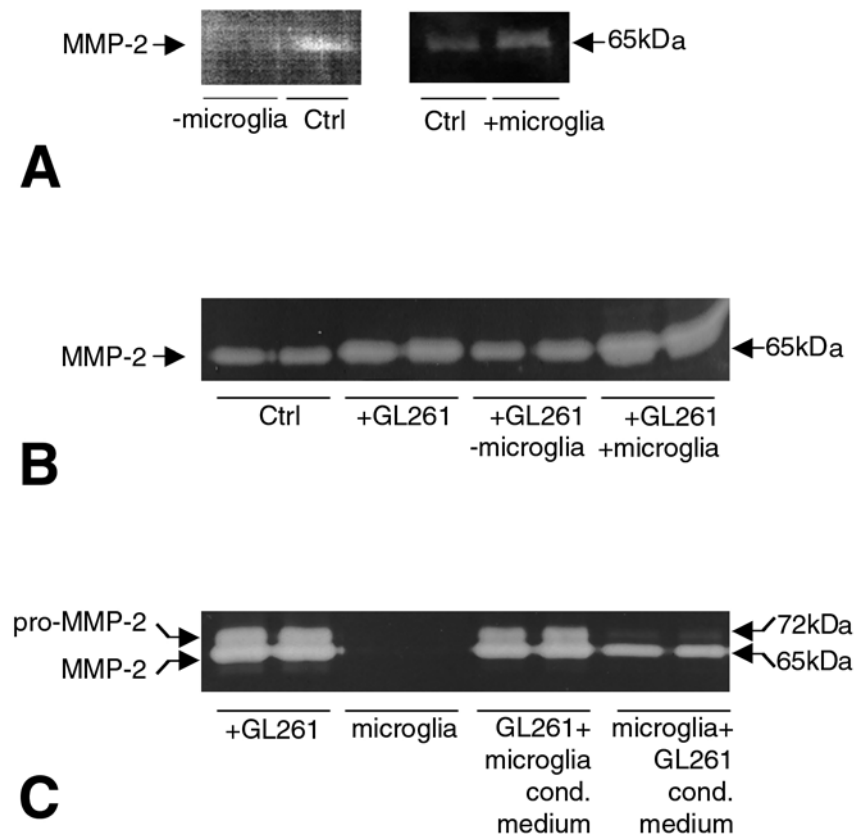


**Fig. 3.11. Supernatant from glioma induce MMP-2 activation by microglia.** (A) Tissue extracts from microglia depleted and control organotypical brain slice cultures inoculated with GL261 cells were analysed for metalloproteinase activity by gelatine zymography. On the right panel the zymography from control organotypical brain slice cultures injected with GL261 only were compared to organotypical brain slice cultures coinjected with microglia. The arrows indicate the presumed molecular weight of MMP-2 and reference markers. (B) Gelatin zymography for metalloproteinase activities was analyzed from supernatant obtained from organotypical brain slice cultures. Control organotypical brain slice cultures were compared with organotypical brain slice cultures injected with GL261 cells (+GL261), microglia-depleted organotypical brain slice cultures (-microglia), or organotypical brain slice cultures coinjected with GL261 and microglial cells (+microglia). (C) Gelatin zymography for metalloproteinase activities was analyzed from supernatant obtained from GL261 and microglial cultures stimulated with GL261 or microglia conditioned media.

### 3.3.3. Microglia activates MMP-2

To determine which process is responsible for release of active MMP-2 from microglia (Fig. 3.11.), the protein synthesis was blocked in microglia with Cycloheximide (CHX) and microglia was stimulated with GL261 conditioned medium (Fig. 3.12.). As Fig. 3.12. illustrates, the activity of MMP-2 from microglia does not depend on de novo protein synthesis. Hence, the proMMP-2 protease released from GL261 cells is activated on the microglial surface.

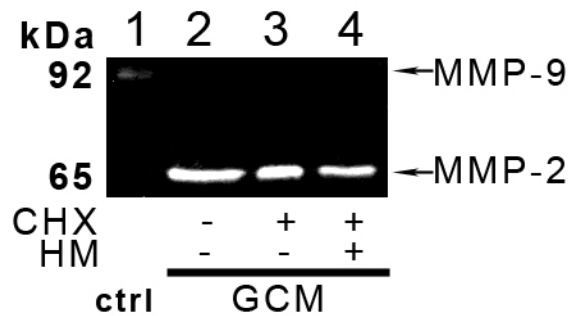


**Fig. 3.12. ProMMP-2 from GL261 cells is activated by microglia.** Microglial release of gelatinases into serum free DMEM- harvesting medium (HM), was assayed by gelatine zymography. Lane 1 demonstrates the basal release of MMP-9 and MMP-2 from the control microglia, where HM was assayed for basal release of gelatinases, and only faint MMP-9 activity was detected. Lane 2 shows as previously described increased release of active MMP-2 after incubation in GCM. In Lane 3 MMP-2 activity persists although the GL261 conditioned medium (GCM) contained 0,1 $\mu$ M CHX. Lane 4 shows activity of MMP-2 when 0,1 $\mu$ M CHX was added to HM.

### 3.3.4. Iba-1 positive cells are accumulating at experimental gliomas

GL261 EGFP cells were injected into the caudate putamen of postnatal day 25 (P25) old mice in order to study the ability of microglia to infiltrate experimental gliomas in vivo. Two weeks post inoculation the mice were sacrificed and their brains were sectioned and immunolabeled for Iba-1, a microglial/macrophage marker. In the non-injected hemisphere Iba-1 positive cells were found evenly dispersed throughout the brain parenchyma (Fig. 3.13A). These microglia exhibited a ramified morphology, indicating a non-activated resting state. Conversely, in the glioma injected hemisphere, we found an increased number of microglial cells (Fig. 3.13B). Microglia were in close contact with GL261 cells and were most abundantly present at the tumor border (Fig. 3.13 C-D). Microglial morphology at the tumor was amoeboid compared to the microglia with their ramified morphology in the contra-lateral (non-injected) hemisphere. Thus, glioma-associated microglia had enlarged cell bodies and it exhibited rather a amoeboid than ramified morphology.

### 3.3.5. The expression of MT1-MMP is increased in microglia surrounding gliomas

Immunolabelling of mouse brain sections for MT1-MMP expression, revealed that MT1-MMP co-localized much stronger with the microglia marker Iba-1 than with GL261 cells (Fig. 3.13C-D). Interestingly, the MT1-MMP labelling of microglia is

stronger when they are in direct contact with GL261 cells. Conversely, MT1-MMP expression exhibited much lower levels in the non-injected hemisphere (Fig. 3.13.A).

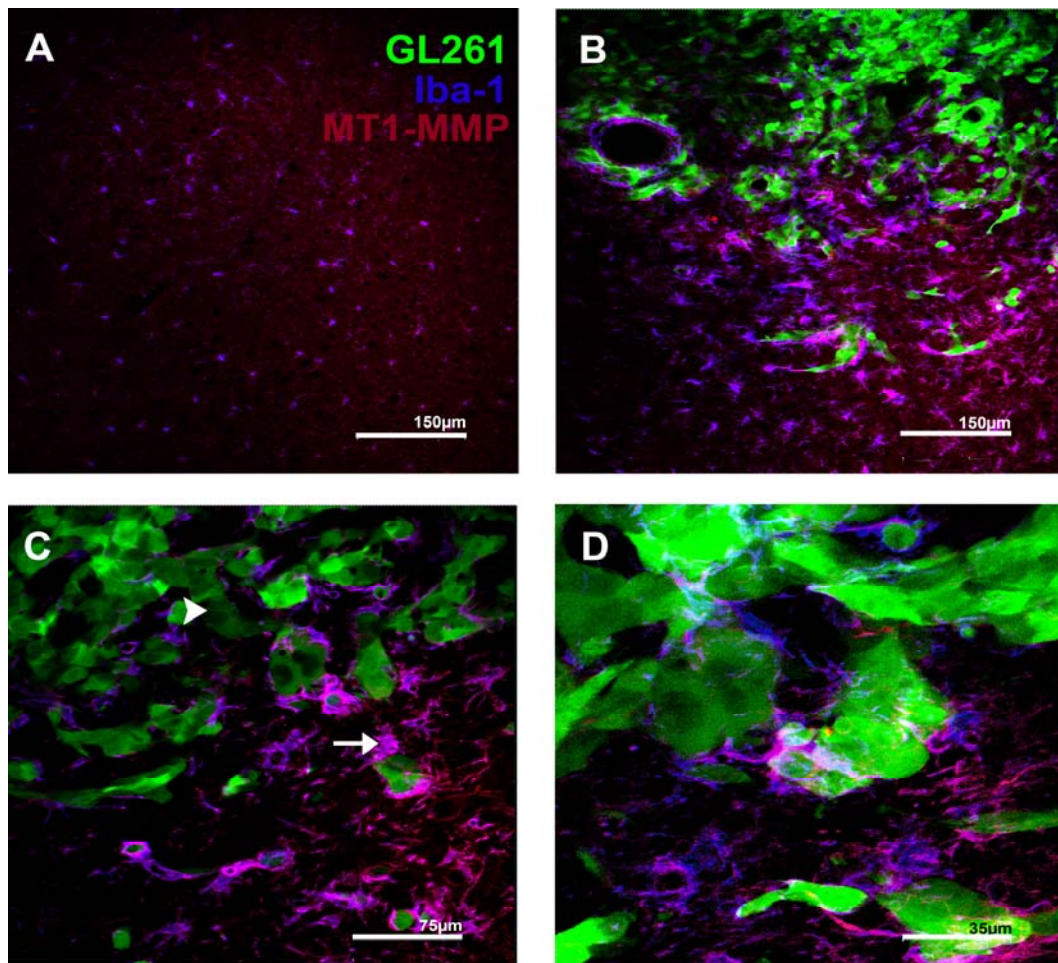


**Fig. 3.13. Iba-1 positive cells overexpress MT1-MMP when associated with experimental gliomas.** Mouse brains were injected with GL261 EGFP (green) cells. Two weeks after the operation the brains were sectioned into 40 $\mu$ m thick slices and labeled for Iba-1 (blue) and MT1-MMP (red). (A) In the control (non- injected) hemisphere, the distribution of Iba-1 positive cells is uniform and the microglia exhibit an amoeboid morphology. The level of MT1-MMP expression is low. (B) The amount of microglia is increased in the vicinity of gliomas. (C-D) Microglia exhibit an amoeboid morphology and associate with gliomas. (C) MT1-MMP expression is increased in the vicinity of glioma, especially in microglia contacting glioma cells (arrow), whereas GL261 are expressing low levels of MT1-MMP (arrowhead). (D) Detail from (C) showed in larger magnification.

### 3.3.6. Microglial expression of MT1-MMP is up- regulated after stimulation with GL261 conditioned medium (GCM)

Since an increased activity of MMP-2 release was observed from microglial cultures upon treatment with glioma conditioned medium and MT1-MMP overexpression in glioma-associated microglia in vivo (Fig. 3.11, 3.12 and 13.13) I was interested in the pathophysiological role of these events. I performed RT-PCR and Western blot analysis of microglial cells which were treated with GL261 conditioned medium.

MT1-MMP was up-regulated after 3h and 6h stimulation with GL261 conditioned medium on the mRNA and protein level. RT-PCR analysis showed that the mRNA of MT1-MMP is up-regulated in microglia after 3 and 6h of stimulation with GCM stimulation (Fig. 3.14A).

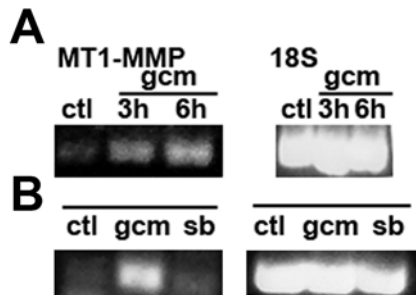


**Fig. 3.14. Transcription of MT1-MMP after GL261 conditioned medium (GCM) treatment is up-regulated.** The microglial cultures were stimulated with GCM or with GCM containing a specific blocker for p38 kinase (SB 202190; sb) RT-PCR analysis of MT1-MMP mRNA in microglia after GCM treatment. (A) GCM treatment increases MT1-MMP mRNA. (B) SB 202190 blocks the induction of MT1-MMP mRNA by GCM.

The active forms of MT1-MMP (57kDa) are overexpressed in microglia treated for 3h and 6h with GCM. Fragments of degraded MT1-MMP are also increased, indicating a higher turnover activity of the active MT1-MMP form after stimulation with GCM (Fig. 3.15).

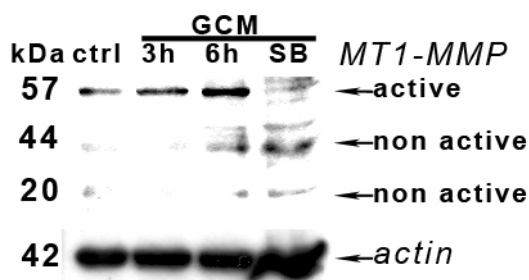


**Fig. 3.15. Increased protein expression and turn-over of MT1-MMP after GL261 conditioned medium (GCM) stimulation.** The microglial cultures were stimulated with GCM or with GCM plus a specific blocker for p38 kinase (SB 202190; SB). Western blots of microglial protein extracts indicate low basal expression under control conditions and an increased activity of MT1-MMP upon a stimulation with GCM. The blots are indicating increased expression and turnover of MT1-MMP in the two central lines. Note blocked expression of MT1-MMP after the treatment with SB 202190.

Finally, it was tested whether the MAPK pathway is mediating the signal from a GL261 released factor to induce up-regulation of MT1-MMP in microglia. It was discovered that the p38 MAPK is involved in inducing the increased expression of MT1-MMP. Stimulation of microglia with GCM containing 5 $\mu$ M SB202190, a p38

MAPK blocker suppresses the expression of MT1-MMP at mRNA and protein levels as shown in Fig. 3.14B and Fig. 3.15 (lanes labelled with sb).

### 3.3.7. The MT1-MMP activity is increased after stimulation with GL261 conditioned medium (GCM)

Only the active form of MT1-MMP is able to activate MMP-2. To assess the amount of active MT1-MMP in microglia after GCM treatment (Fig. 3.14 and 3.15) an MT1-MMP activity assay was used. This indirect assay measures urokinase activity, an enzyme that is cleaved and released by active MT1-MMP. The MT1-MMP activity in microglia was significantly elevated 3h and 6h after incubation with GCM (Fig. 16). 6h after treatment with GCM the activity of MT1-MMP was three times larger as compared to control microglia, whereas, SB202190 reduced the activity after GCM treatment of microglia. Statistically significant differences in MT1-MMP activity appeared after 3 and 6 hours stimulation with GCM. The enzymatic activity was increased by 148% and 293% after 3 and 6 hours, respectively. However, combination treatment of GCM and SB202190 largely abrogated the up-regulation of active MT1-MMP, after three and six hours treatment.

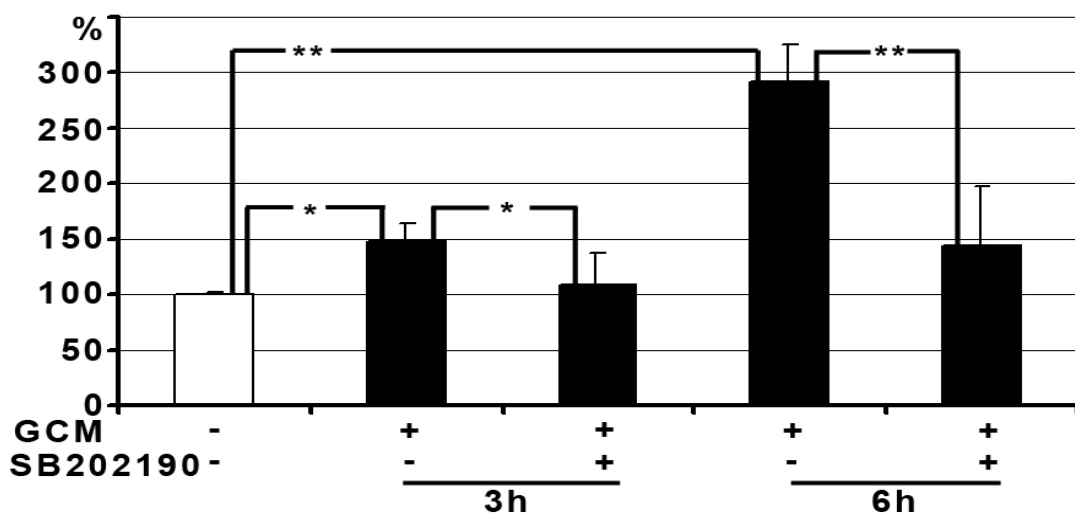


**Fig. 3.16. MT1-MMP activity increase after GL261 conditioned medium (GCM) treatment is mediated by p38 MAPK.** Microglial cultures were stimulated with GCM or with GCM containing the specific blocker of p38 MAPK, SB 202190, for indicated time periods. Activity of MT1-MMP was assayed with Matrix Metalloproteinase-14, Biotrak Activity Assay System (Amersham Biosciences, USA). The activity is expressed in percent and compared to normalized, control (non stimulated) microglia. Statistical significance was indicated with asterisks;  $p < 0,05$  with one and  $p < 0,01$  with two asterisks.